

A FAST HIGH ORDER METHOD FOR ELECTROMAGNETIC SCATTERING BY LARGE OPEN CAVITIES*

Meiling Zhao

School of Mathematics and System Science, Beijing University of Aeronautics & Astronautics, Beijing 100191, China

Email: meilingzhaocn@yahoo.com

Zhonghua Qiao*

Institute for Computational Mathematics & Department of Mathematics, Hong Kong Baptist University, Kowloon, Hong Kong

Email: zqiao@hkbu.edu.hk

Tao Tang

Department of Mathematics, Hong Kong Baptist University, Kowloon, Hong Kong

Email: ttang@hkbu.edu.hk

Abstract

In this paper, the electromagnetic scattering from a rectangular large open cavity embedded in an infinite ground plane is studied. By introducing a nonlocal artificial boundary condition, the scattering problem from the open cavity is reduced to a bounded domain problem. A compact fourth order finite difference scheme is then proposed to discretize the cavity scattering model in the rectangular domain, and a special treatment is enforced to approximate the boundary condition, which makes truncation errors reach $\mathcal{O}(h^4)$ in the whole computational domain. A fast algorithm, exploiting the discrete Fourier transformation in the horizontal and a Gaussian elimination in the vertical direction, is employed, which reduces the discrete system to a much smaller interface system. An effective preconditioner is presented for the BICGstab iterative solver to solve this interface system. Numerical results demonstrate the remarkable accuracy and efficiency of the proposed method. In particular, it can be used to solve the cavity model for the large wave number up to 600π .

Mathematics subject classification: 65N06, 78M20.

Key words: Electromagnetic cavity, Compact finite difference scheme, FFT, Preconditioning.

1. Introduction

The scattering properties of open cavities are of high interest to the engineering community, with a number of applications including the design of jet engine inlet ducts and cavity-backed antenna for military and civil use. In this paper we mainly concern with the electromagnetic scattering from a two-dimensional large open cavity as shown in Fig. 1.1. The ground plane and the walls of the open cavity are assumed as perfect electric conductors (PEC), and the interior of the open cavity is filled with non-magnetic materials which may be inhomogeneous. The half space above the ground plane is filled with a homogenous and isotropic medium with its permittivity ε_0 and permeability μ_0 . In this setting, the electromagnetic scattering by the

* Received January 16, 2010 / Revised version received June 1, 2010 / Accepted July 20, 2010 /
Published online February 28, 2011 /

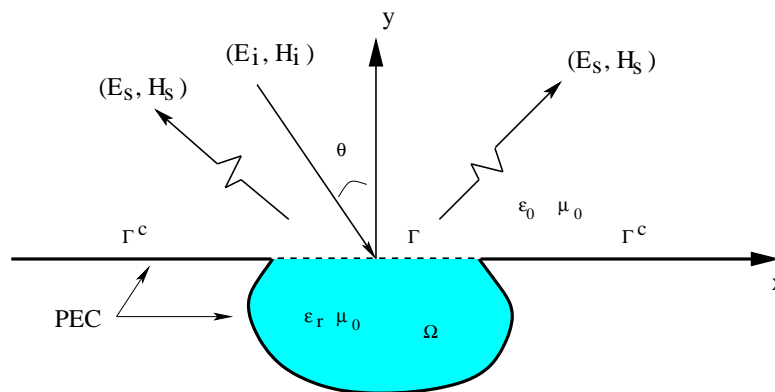


Fig. 1.1. The geometry of the cavity.

cavity is governed by the Helmholtz equation along with Sommerfeld's radiation conditions imposed at infinity. A variety of numerical methods, including the method of moments, finite difference, finite element, boundary element method, and hybrid methods [3, 7, 9, 10], have been developed to characterize the scattering from cavities. Some mathematical analysis and numerical treatments on the open cavities can be found in [1, 2, 5].

However, the problem will be challenging when the wave number k is large, or the cavity becomes large compared to the wavelength of the fields, more precisely large ka , where a denotes the size of the computational domain, because of the highly oscillatory nature of the fields. For a large wave number, the phase error (pollution) of the computed solution obtained with low order discretization is large unless fine meshes are used per wavelength. See [22] for detailed information. A fine mesh would lead to a large system of equations which may be computationally prohibitive. For instance, a large cavity, $1\text{m} \times 1\text{m}$, with a centimeter incident wave, this condition means when choosing mesh density as $1/20 \sim 1/40$ of the wavelength, it will produce 10^8 unknowns in the discrete linear systems of the two-dimensional case. Many numerical approaches have been proposed to reduce the phase error. For example, the high-order finite element method was proposed in [7]; the h -version and h - p -version finite element methods were proposed in [23, 24]. In [11], a standard bilinear finite element together with a modified quadrature rule was used, which led to fourth order phase accuracy on orthogonal uniform meshes. The high order spectral method and compact high order finite difference method have been presented to solve the Helmholtz equation in [12, 13, 16–18, 25]. In [8], a fully high-order finite element with curvilinear tetrahedral elements was developed to simulate the scattering by cavities. High order methods are attractive for solving the Helmholtz problem with the large wave number since they can offer relative higher accurate solution by utilizing fewer mesh points and spending less computational costs than the low order approaches.

For the cavity electromagnetic scattering problem, the accurate computation for the radar cross section (RCS) is of particular importance. Bao and Sun proposed a fast algorithm in [3] for solving the electromagnetic scattering from a rectangular cavity. Using the discrete Fourier transform in the horizontal direction and a Gaussian elimination in the vertical direction, the approach reduces the global system in the entire cavity to an interface linear system on the top line of the cavity with computational complexity proportional to the number of the unknowns by appropriate iterative methods in the source free case. This algorithm was further improved in [14].

In this work, we propose a fast high order finite difference method for the scattering of

electromagnetic plane waves by a two-dimensional (2-D) rectangular cavity in the infinite ground plane. According to the fact that a straightforward change of coordinates yields the equivalence of the large wave number and large cavity problems in current context, we emphasize the case in the large wave number in the discussion. In the cavity domain, the compact four order finite difference scheme is used for the discretization of the equation, and at the aperture, a fourth order approximation is also designed by a special technique. Following the work in [3,14], a fast algorithm, utilizing the discrete Fourier transform in the horizontal direction and the Gaussian elimination in the vertical direction, is presented to solve the resulting discrete system. An interface linear system is formed by reducing the global system. For relatively large wave numbers, the reduced interface linear system may be ill-conditioned. So we present an effective preconditioner for the BICGstab iterative solver, which further increases the performance and capability of our high order method. Numerical experiments are carried out to verify the efficiency of the presented high order method.

The rest of the paper is organized as follows. In the next section, the scattering model from open cavity is stated and further is reduced to a bounded domain problem. In Section 3, the fast high order method is presented. Numerical experiments are presented to illustrate the competitive behavior of the method in Section 4. The paper ends with some conclusions in the last section.

2. Two-Dimensional Open Cavity Model

We consider the plane wave scattering problem by a open cavity embedded in an infinite ground plane as in Fig. 1.1. The ground plane and cavity wall are perfect electric conductors (PEC). Assume that the medium and material is invariant in the z -direction. Throughout the paper, the media are assumed to be nonmagnetic, having relative magnetic permeability $\mu_r = 1$. The interior of the cavity may be filled with inhomogeneous materials having relative electric permittivity $\varepsilon_r(x, y)$. We are interested in the scattering of an incident plane wave by the cavity.

Let us denote $\Omega \in R^2$ as the cavity embedded in the ground plane with boundary $\partial\Omega$, which consists of the cavity aperture Γ and the cavity wall $\partial\Omega \setminus \Gamma$. Let R_+^2 be the region above the ground plane $\{(x, y) \in R^2 : y > 0\}$. $\partial R_+^2 \setminus \Gamma$ is the ground plane without the aperture.

For the transverse magnetic (TM) case, in which the magnetic field is transverse to the invariant direction and the incident electric field and the total electric field are parallel to the invariant dimension, i.e., $E_I = (0, 0, u^i)$ and $E_{tot} = (0, 0, u)$. By the electric continuity conditions, u vanishes on the cavity walls and on the ground plane except over the aperture Γ . The time-harmonic Maxwell equation is reduced to

$$\Delta u + k^2 u = f(x, y), \quad (x, y) \in \Omega \cup R_+^2, \quad (2.1a)$$

$$u = 0, \quad \text{on } \Gamma^c \cup (\partial\Omega \setminus \Gamma), \quad (2.1b)$$

together with the radiation boundary condition

$$\lim_{r \rightarrow \infty} \sqrt{r} \left(\frac{\partial u^s}{\partial r} - ik_0 u^s \right) = 0. \quad (2.2)$$

where u^s is the tangential component of the scattered field $E_S = (0, 0, u^s)$, and $k^2 = \omega^2 \varepsilon \mu = k_0^2 \varepsilon_r \mu_r$. We assume that $\varepsilon = \varepsilon(y)$ only depends on the variable y . The fields are said to be source free if the source term $f = 0$.

Assume that a plane wave $u^i = e^{i(\alpha x - \beta y)}$ is incident on the cavity from above, where $\alpha = k_0 \sin \theta$, $\beta = k_0 \cos \theta$, and $-\pi/2 < \theta < \pi/2$ is the angle of incident with respect to the positive y -axis. The scattered field u^s can be expressed by $u^s = u - u^i + e^{i(\alpha x + \beta y)}$. Clearly, u^s satisfies

$$\Delta u^s + k_0^2 u^s = 0, \quad (x, y) \in R_2^+, \tag{2.3a}$$

$$u^s = u(x, 0), \quad \text{on } \Gamma, \tag{2.3b}$$

$$u^s = 0, \quad \text{on } \Gamma^c. \tag{2.3c}$$

By using the Green's theorem, we have

$$u^s(\mathbf{x}) = \int_{\Gamma} \left\{ \frac{\partial G_d(\mathbf{x}, \mathbf{x}')}{\partial y'} u^s(\mathbf{x}') \right\}_{y'=0^+} dx'. \tag{2.4}$$

In (2.4), $G_d(\mathbf{x}, \mathbf{x}')$ is the upper half-plane Dirichlet Green's function for the Helmholtz equation

$$G_d(\mathbf{x}, \mathbf{x}') = \frac{i}{4} [H_0^1(k_0|\mathbf{x} - \mathbf{x}'|) - H_0^1(k_0|\mathbf{x} - \bar{\mathbf{x}}'|)],$$

where $\mathbf{x} = (x, y)$ and $\mathbf{x}' = (x', y')$ denote source point and field point separately, and $\bar{\mathbf{x}}'$ is the image of \mathbf{x}' with respect to the real axis. By the boundary conditions and the field continuity, the total field u satisfies the condition on Γ

$$\frac{\partial u}{\partial y} \Big|_{y=0^+} = I(u) + g(x), \quad x \in \Gamma,$$

where

$$I(u) = \frac{ik_0}{2} \int_{\Gamma} \frac{1}{|x - x'|} H_1^{(1)}(k_0|x - x'|) u(x', 0) dx'$$

is called the nonlocal boundary condition or the transparent boundary condition, and $g(x) = -2i\beta e^{i\alpha x}$, $x \in \Gamma$. Consequently, the scattering problem can be reduced to a bounded problem:

$$\Delta u + k^2 u = f(x, y), \quad (x, y) \in \Omega, \tag{2.5a}$$

$$u = 0, \quad \text{on } \partial\Omega \setminus \Gamma, \tag{2.5b}$$

$$\frac{\partial u}{\partial n} = I(u) + g(x), \quad \text{on } \Gamma. \tag{2.5c}$$

In the TE case, the formulation process can be similarly deduced (see, e.g., [3]), and the total field satisfies

$$\nabla \cdot \left(\frac{1}{\varepsilon_r} \nabla u \right) + k_0^2 \mu_r u = f(x, y), \quad (x, y) \in \Omega, \tag{2.6a}$$

$$\frac{\partial u}{\partial n} = 0, \quad \text{on } \partial\Omega \setminus \Gamma, \tag{2.6b}$$

$$u = \tilde{I}(u) + \tilde{g}(x), \quad \text{on } \Gamma, \tag{2.6c}$$

where

$$\tilde{I}(u) = -\frac{i}{2} \int_{\Gamma} \frac{1}{\varepsilon_r(x')} H_0^1(k_0|x' - x|) \frac{\partial u(x', y')}{\partial y'} \Big|_{y'=0^-} dx', \quad \tilde{g}(x) = 2e^{i\alpha x}.$$

3. Fast High Order Algorithm

In this section we shall introduce a fast fourth order compact method for the scattering problem from open rectangular cavities, and take the case of TM Polarization as example. The algorithm in TE case can be similarly formulated.

3.1. Compact fourth order scheme

Let $\{x_i, y_j\}_{i,j=0}^{M+1,N+1}$ define a uniform partition of $\Omega = [0, a] \times [-b, 0]$. For ease of notations, we only consider $\Delta x = \Delta y = h$, and the main ideas in this work can be extended to rectangular cavities with $\Delta x \neq \Delta y$. Using the notation

$$\delta_x^2 u_{i,j} = \frac{u_{i-1,j} - 2u_{i,j} + u_{i+1,j}}{h^2}, \quad \delta_y^2 u_{i,j} = \frac{u_{i,j-1} - 2u_{i,j} + u_{i,j+1}}{h^2}, \tag{3.1}$$

the discrete finite difference system in the TM case can be given by

$$\begin{aligned} & \left(1 + \frac{k^2(y)h^2}{12}\right) (\delta_x^2 + \delta_y^2)u_{i,j} + \frac{h^2}{6}\delta_x^2\delta_y^2u_{i,j} + k^2(y)u_{i,j} \\ & = f_{i,j} + \frac{h^2}{12}(\delta_x^2 + \delta_y^2)f_{i,j}, \quad i = 1, \dots, M, \quad j = 1, \dots, N, \end{aligned} \tag{3.2}$$

or in matrix form,

$$\begin{aligned} & \left((I_{MN} + \frac{h^2}{12}(I_M \otimes D))(A_M \otimes I_N + I_M \otimes A_N) + \frac{h^2}{6}(A_M \otimes A_N) + I_M \otimes D \right) U_1 \\ & + \left((I_{MN} + \frac{h^2}{12}(I_M \otimes D))(I_M \otimes a_N) + \frac{h^2}{6}(A_M \otimes a_N) \right) u_{:,N+1} \\ & = \frac{h^2}{12}(A_M \otimes I_N + I_M \otimes A_N)F_1 + \frac{1}{12} \begin{pmatrix} I_N \\ \mathbf{0} \end{pmatrix} f_{0,:} + \frac{1}{12} \begin{pmatrix} \mathbf{0} \\ I_N \end{pmatrix} f_{M+1,:} \\ & + \frac{1}{12}(I_M \otimes b_N)f_{:,0} + \frac{1}{12}(I_M \otimes a_N)f_{:,N+1} + I_{MN}F_1, \end{aligned} \tag{3.3}$$

where \otimes denotes the tensor product (Kronecker product), I_{MN} is the $MN \times MN$ identity matrix, and I_M is the $M \times M$ identity matrix,

$$\begin{aligned} A_M &= \frac{1}{h^2} \begin{pmatrix} -2 & 1 & & \\ 1 & -2 & 1 & \\ & \ddots & \ddots & \ddots \\ & & & 1 & -2 \end{pmatrix}, \quad A_N = \frac{1}{h^2} \begin{pmatrix} -2 & 1 & & \\ 1 & -2 & 1 & \\ & \ddots & \ddots & \ddots \\ & & & 1 & -2 \end{pmatrix}, \\ D &= \omega^2 \mu_0 \begin{pmatrix} \varepsilon(y_1) & & & \\ & \varepsilon(y_2) & & \\ & & \ddots & \\ & & & \varepsilon(y_N) \end{pmatrix}, \quad a_N = \frac{1}{h^2} \begin{pmatrix} 0 \\ \vdots \\ 0 \\ 1 \end{pmatrix}, \quad b_N = \frac{1}{h^2} \begin{pmatrix} 1 \\ 0 \\ \vdots \\ 0 \end{pmatrix}, \end{aligned}$$

and

$$\begin{aligned} U_1 &= (u_{11}, \dots, u_{1N}, u_{21}, \dots, u_{2N}, \dots, u_{M1}, \dots, u_{MN})^T, \\ u_{:,N+1} &= (u_{1,N+1}, u_{2,N+1}, \dots, u_{M,N+1}), \\ F_1 &= (f_{11}, \dots, f_{1N}, f_{21}, \dots, f_{2N}, \dots, f_{M1}, \dots, f_{MN})^T. \end{aligned}$$

A_M is an $M \times M$ matrix, and A_N is an $N \times N$ matrix. a_N and b_N are also N dimensional vectors. $f_{0,:}$, $f_{M+1,:}$ and $f_{:,0}$, $f_{:,N+1}$ denote the vectors when $x = 0, 1$ and $y = 0, 1$ respectively.

For the tridiagonal Toeplitz matrix A_M , we have

$$S_M A_M S_M = \Lambda = \text{diag}(\lambda_1, \lambda_2, \dots, \lambda_M),$$

where S_M denotes the discrete Fourier-sine transformation,

$$(S_M)_{l,m} = \sqrt{\frac{2}{M+1}} \sin \frac{lm\pi}{M+1}, \quad \lambda_l = -\frac{4(M+1)^2}{a^2} \sin^2 \frac{l\pi}{2(M+1)}, \quad 1 \leq l, \quad m \leq M,$$

and $S_M^2 = I_M$. Using the discrete Fourier sine transformation, the discrete system (3.3) can be written as

$$\begin{aligned} & \left((I_{MN} + \frac{h^2}{12}(I_M \otimes D))(\Lambda \otimes I_N + I_M \otimes A_N) + \frac{h^2}{6}(\Lambda \otimes A_N) + I_M \otimes D \right) \bar{U}_1 \\ & + \left((I_{MN} + \frac{h^2}{12}(I_M \otimes D))(I_M \otimes a_N) + \frac{h^2}{6}(\Lambda \otimes a_N) \right) \bar{u}_{:,N+1} \\ & = \frac{h^2}{12} \left(\Lambda \otimes I_N + I_M \otimes A_N + \frac{12}{h^2} I_N \right) \bar{F}_1 + \frac{1}{12} (S_{:,1} \otimes I_N) f_{0,:} + \frac{1}{12} (S_{:,M} \otimes I_N) f_{M+1,:} \\ & + \frac{1}{12} (I_M \otimes b_N) \bar{f}_{:,0} + \frac{1}{12} (I_M \otimes a_N) \bar{f}_{:,N+1}, \end{aligned} \tag{3.4}$$

where

$$\begin{aligned} \bar{U}_1 &= (S_M \otimes I_N) U_1 = (\bar{u}_{1,1}, \dots, \bar{u}_{1,N}, \bar{u}_{2,1}, \dots, \bar{u}_{2,N}, \dots, \bar{u}_{M,1}, \dots, \bar{u}_{M,N}), \\ \bar{u}_{:,N+1} &= S_M u_{:,N+1}, \quad \bar{F}_1 = (S_M \otimes I_N) F_1, \quad \bar{f}_{:,0} = S_M f_{:,0}, \quad \bar{f}_{:,N+1} = S_M f_{:,N+1}. \end{aligned}$$

$S_{:,1}$ and $S_{:,M}$ are the first column vector and the last one of S_M separately. Eq. (3.4) can be further rewritten as

$$\begin{aligned} & \left((I_N + \frac{h^2}{12}D)(A_N + \lambda_i I_N) + \frac{h^2}{6} \lambda_i A_N + D \right) \bar{u}_{i,:} + \left((I_N + \frac{h^2}{12}D)a_N + \frac{h^2}{6} \lambda_i a_N \right) \bar{u}_{i,N+1} \\ & = \frac{h^2}{12} \left(\lambda_i I_N + A_N + \frac{12}{h^2} I_N \right) \bar{F}_{i,:} + \frac{1}{12} S_{i,1} I_N f_{0,:} + \frac{1}{12} S_{i,M} I_N f_{M+1,:} \\ & + \frac{1}{12} I_B \bar{f}_{i,0} + \frac{1}{12} I_A \bar{f}_{i,N+1}, \quad i = 1, \dots, M, \end{aligned} \tag{3.5}$$

where $(I_A)_{ij} = 0$ except $(I_A)_{11} = 1$; $(I_B)_{ij} = 0$ except $(I_B)_{M,1} = 1$, $1 \leq i, j \leq M$. $S_{i,1}$ and $S_{i,M}$ are the $i1$ and iM entry of the matrix S_M .

We use the forward Gaussian elimination method with a row partial pivoting to solve each system in (3.5). Let

$$\left(I_N + \frac{h^2}{12}D \right) (A_N + \lambda_i I_N) + \frac{h^2}{6} \lambda_i A_N + D = L_i U_i, \quad i = 1, \dots, M$$

be the LU -decomposition, where

$$\left(I_N + \frac{h^2}{12}D \right) (A_N + \lambda_i I_N) + \frac{h^2}{6} \lambda_i A_N + D$$

is a symmetric tridiagonal matrix. The last equations of the system (3.5) can be written as

$$\alpha_i \bar{u}_{iN} + \beta_i \bar{u}_{i,N+1} = \hat{f}_{iN}, \quad i = 1, \dots, M, \tag{3.6}$$

where α_i is the last component of U_i , β_i is the last element of

$$L_i^{-1} \left((I_N + \frac{h^2}{12}D)a_N + \frac{h^2}{6}\lambda_i a_N \right),$$

and \widehat{f}_{iN} is the right-hand term of the last systems of (3.5) multiplied by L_i^{-1} . Eq. (3.6) is equivalent to

$$D_\alpha \bar{u}_{:,N} + D_\beta \bar{u}_{:,N+1} = \widehat{f}_{:,N}, \tag{3.7}$$

where $D_\alpha = \text{diag}(\alpha_1, \alpha_2, \dots, \alpha_M)$, $D_\beta = \text{diag}(\beta_1, \beta_2, \dots, \beta_M)$.

3.2. Fourth order approximation of the nonlocal boundary condition

Next we introduce the fourth order approximation of the nonlocal boundary condition. Using the Taylor expansion at (x_i, y_{N+1}) , we can obtain

$$\begin{aligned} \frac{u_{i,N+2} - u_{iN}}{2h} &= (u_y)_{i,N+1} + \mathcal{O}(h^2) \\ &= \sum_{l=1}^M G_{il} u_{l,N+1} + g(x_i) + \mathcal{O}(h^2), \quad i = 1, \dots, M, \end{aligned}$$

where $\sum_{l=1}^M G_{il} u_{l,N+1}$ is the approximation of the hypersingular integration in (2.5a), and it can be calculated numerically (see in [15]).

Assuming f is sufficiently smooth in $\bar{\Omega}$ and adding the (3.2) on the boundary Γ , we have

$$\begin{aligned} &\frac{u_{i,N+2} - u_{iN}}{2h} \\ &= (u_y)_{i,N+1} + \frac{h^2}{6} (f_y - k^2(y)u_y - u_{xxy})_{i,N+1} + \mathcal{O}(h^4) \\ &= Gu_{i,N+1} + g_i + \frac{h^2}{6} (f_y)_{i,N+1} - \frac{k^2(y)h^2}{6} \frac{u_{i,N+2} - u_{i,N}}{2h} - \frac{h^2}{6} \frac{\delta_x^2 u_{i,N+2} - \delta_x^2 u_{i,N}}{2h} + \mathcal{O}(h^4), \end{aligned}$$

which leads to a fourth order approximation expression for the boundary condition $\frac{\partial u}{\partial n} = I(u) + g(x)$,

$$\begin{aligned} &\left(1 + \frac{k^2(y)h^2}{6} \right) \frac{u_{i,N+2} - u_{iN}}{2h} + \frac{h^2}{6} \frac{\delta_x^2 u_{i,N+2} - \delta_x^2 u_{i,N}}{2h} - Gu_{i,N+1} \\ &= g_i + \frac{h^2}{6} (f_y)_{i,N+1}, \end{aligned} \tag{3.8}$$

or in matrix form

$$\begin{aligned} &\left(I_M + \frac{h^2}{6}D_0 + \frac{h^2}{6}A_M \right) u_{:,N+2} - \left(I_M + \frac{h^2}{6}D_0 + \frac{h^2}{6}A_M \right) u_{:,N} \\ &= 2hGu_{:,N+1} + 2hg + \frac{h^3}{3}(f_y)_{:,N+1}, \end{aligned} \tag{3.9}$$

where $D_0 = \text{diag}(k^2(y_{N+1}), k^2(y_{N+1}), \dots, k^2(y_{N+1}))$, and D_0 is M dimensional diagonal matrix. Multiplied by S_M , the above equation will turn into

$$\begin{aligned} &S_M \left(I_M + \frac{h^2}{6}D_0 + \frac{h^2}{6}A_M \right) S_M \bar{u}_{:,N+2} - S_M \left(I_M + \frac{h^2}{6}D_0 + \frac{h^2}{6}A_M \right) S_M \bar{u}_{:,N} \\ &= 2hS_MGS_M \bar{u}_{:,N+1} + 2hS_Mg + \frac{h^3}{3}S_M(f_y)_{:,N+1}, \end{aligned} \tag{3.10}$$

where $\bar{u}_{:,N+2} = S_M u_{:,N+2}$, $\bar{u}_{:,N} = S_M u_{:,N}$. Equivalent to the following equation

$$\begin{aligned} & \left(I_M + \frac{h^2}{6} D_0 + \frac{h^2}{6} \Lambda \right) \bar{u}_{:,N+2} - \left(I_M + \frac{h^2}{6} D_0 + \frac{h^2}{6} \Lambda \right) \bar{u}_{:,N} \\ &= 2h S_M G S_M \bar{u}_{:,N+1} + 2h S_M g + \frac{h^3}{3} S_M (f_y)_{:,N+1}. \end{aligned} \tag{3.11}$$

We can get the $\bar{u}_{:,N+2}$

$$\begin{aligned} \bar{u}_{:,N+2} &= \bar{u}_{:,N} + 2h \left(I_M + \frac{h^2}{6} D_0 + \frac{h^2}{6} \Lambda \right)^{-1} S_M G S_M \bar{u}_{:,N+1} \\ &+ 2h \left(I_M + \frac{h^2}{6} D_0 + \frac{h^2}{6} \Lambda \right)^{-1} S_M g + \frac{h^3}{3} \left(I_M + \frac{h^2}{6} D_0 + \frac{h^2}{6} \Lambda \right)^{-1} S_M (f_y)_{:,N+1}. \end{aligned} \tag{3.12}$$

To eliminate the values of u at the ghost points, we add the difference equation on (3.2) at the boundary points $(x_i, y_{N+1}) (1 \leq i \leq M)$,

$$\begin{aligned} & \left(1 + \frac{k^2(y)h^2}{12} \right) (\delta_x^2 + \delta_y^2) u_{i,N+1} + \frac{h^2}{6} \delta_x^2 \delta_y^2 u_{i,N+1} + k^2(y) u_{i,N+1} \\ &= f_{i,N+1} + \frac{h^2}{12} \Delta f_{i,N+1}. \end{aligned} \tag{3.13}$$

or in matrix form

$$\begin{aligned} & \left(I_M + \frac{h^2}{12} D_0 + \frac{h^2}{6} A_M \right) u_{:,N+2} + \left(I_M + \frac{h^2}{12} D_0 + \frac{h^2}{6} A_M \right) u_{:,N} \\ &+ \left((I_M + \frac{h^2}{12} D_0)(h^2 A_M - 2I_M) - \frac{h^2}{3} A_M + h^2 D_0 \right) u_{:,N+1} \\ &= h^2 f_{:,N+1} + \frac{h^4}{12} \Delta f_{:,N+1}. \end{aligned} \tag{3.14}$$

Multiplied by S_M , we have

$$\begin{aligned} & \left(I_M + \frac{h^2}{12} D_0 + \frac{h^2}{6} \Lambda \right) \bar{u}_{:,N+2} + \left(I_M + \frac{h^2}{12} D_0 + \frac{h^2}{6} \Lambda \right) \bar{u}_{:,N} \\ &+ \left((I_M + \frac{h^2}{12} D_0)(h^2 \Lambda - 2I_M) - \frac{h^2}{3} \Lambda + h^2 D_0 \right) \bar{u}_{:,N+1} \\ &= h^2 S_M f_{:,N+1} + \frac{h^4}{12} S_M \Delta f_{:,N+1}. \end{aligned} \tag{3.15}$$

By eliminating the terms $u_{:,N+2}$ from (3.15) with (3.12), we obtained a fourth order approximation of the transparent boundary Γ as follows,

$$\begin{aligned} & \left((I_M + \frac{h^2}{12} D_0)(h^2 \Lambda - 2I_M) - \frac{h^2}{3} \Lambda + h^2 D_0 + 2h J_2 J_1^{-1} S_M G S_M \right) \bar{u}_{:,N+1} + 2J_2 \bar{u}_{:,N} \\ &= -2h J_2 J_1^{-1} S_M g - \frac{h^3}{3} J_2 J_1^{-1} S_M (f_y)_{:,N+1} + h^2 S_M f_{:,N+1} + \frac{h^4}{12} S_M \Delta f_{:,N+1}, \end{aligned} \tag{3.16}$$

where

$$J_1 = \left(I_M + \frac{h^2}{6} D_0 + \frac{h^2}{6} \Lambda \right), \quad J_2 = \left(I_M + \frac{h^2}{12} D_0 + \frac{h^2}{6} \Lambda \right).$$

Combining (3.16) and (3.7) yields

$$\begin{aligned} & \left(\frac{2}{3}h^2\Lambda + \frac{5}{6}h^2D_0 + \frac{1}{12}h^4D_0\Lambda - 2I_M - 2J_2D_\alpha^{-1}D_\beta + 2hJ_2J_1^{-1}S_MGS_M \right) \bar{u}_{:,N+1} \\ & = -2J_2D_\alpha^{-1}\hat{f}_{:,N} - 2hJ_2J_1^{-1}S_Mg - \frac{h^3}{3}J_2J_1^{-1}S_M(f_y)_{:,N+1} + h^2S_Mf_{:,N+1} + \frac{h^4}{12}S_M\Delta f_{:,N+1}. \end{aligned} \quad (3.17)$$

The rest of the unknowns $\bar{u}_{i,:}, i = 1, 2, \dots, M$ can be obtained by computing Eq. (3.5) with the solved $\bar{u}_{:,N+1}$.

Compared with the second order method in [3, 14], the proposed approach has no increase in the order of the magnitudes in computation complexity, only some addition in the number of matrix multiplication.

3.3. Iterative solution

For relatively large wave number, the system (3.17) will become ill conditioned, which can not be solved by the direct method, such as Gaussian elimination because of the expensive computational spending. The classical iterative algorithms are also less efficient (see Section 4). Thus an effective preconditioner is needed for the iterative method.

Consider the coefficient matrix of (3.17)

$$B = \frac{2}{3}h^2\Lambda + \frac{5}{6}h^2D_0 + \frac{1}{12}h^4D_0\Lambda - 2I_M - 2J_2D_\alpha^{-1}D_\beta + 2hJ_2J_1^{-1}S_MGS_M.$$

Assume D_G is the diagonal matrix composed by the diagonal entries of the imaginary part of G , and let the inverse of

$$M = \frac{2}{3}h^2\Lambda + \frac{5}{6}h^2D_0 + \frac{1}{12}h^4D_0\Lambda - 2I_M - 2J_2D_\alpha^{-1}D_\beta - i2hJ_2J_1^{-1}D_G \quad (3.18)$$

be a preconditioner. Then the system becomes

$$M^{-1}B\bar{u}_{:,N+1} = M^{-1}b,$$

i.e.,

$$\left(I_M + 2hM^{-1}J_2J_1^{-1}(S_MGS_M + iD_GI_M) \right) \bar{u}_{:,N+1} = M^{-1}b, \quad (3.19)$$

where b denotes the right hand term of (3.17).

4. Numerical Experiments

In this section, we consider the plane wave scattering by rectangular cavities. Example 1 and 2 are the artificial problems, which are used to verify the convergence rate of our method. The practical physical model is presented in Example 3. We compute the monostatic RCS of both the unfilled cavity ($\epsilon_r = 1$) and the filled one ($\epsilon_r \neq 1$). The numerical results show the efficiency of the proposed high order method.

4.1. Example 1

An artificial example defined by (2.5a) with a cavity $a = b = 1$ to verify the accuracy of approximations. The $f(x, y)$ and $g(x)$ are chosen such that the exact function is

$$u(x, y) = e^{xy} \sin\left(\frac{k_0x}{2}\right) \sin\left(\left(\frac{k_0}{2} + \frac{\pi}{4}\right)y\right),$$

and $g(x)$ is computed by $g(x) = \frac{\partial u}{\partial n} - I(u)$.

Error measures in L_2 norm and L_∞ norm in the domain Ω are defined by

$$e_M(\Omega) = \max |u_{i,j}^h - u(x_i, y_j)|, \quad e_2(\Omega) = \left(\frac{ab}{M(N+1)} \sum_{i=1}^M \sum_{j=1}^{N+1} |u_{ij}^h - u(x_i, y_j)|^2 \right)^{\frac{1}{2}}$$

separately, where u_{ij}^h denotes the numerical solution at the point (x_i, y_j) . The solution at the aperture of cavity is more interesting for the calculation of RCS, so we also define the following error measures on Γ ,

$$e_M(\Gamma) = \max_i |u_{i,N+1}^h - u(x_i, 0)|, \quad e_2(\Gamma) = \left(\frac{a}{M} \sum_{i=1}^M |u_{i,N+1}^h - u(x_i, 0)|^2 \right)^{\frac{1}{2}}.$$

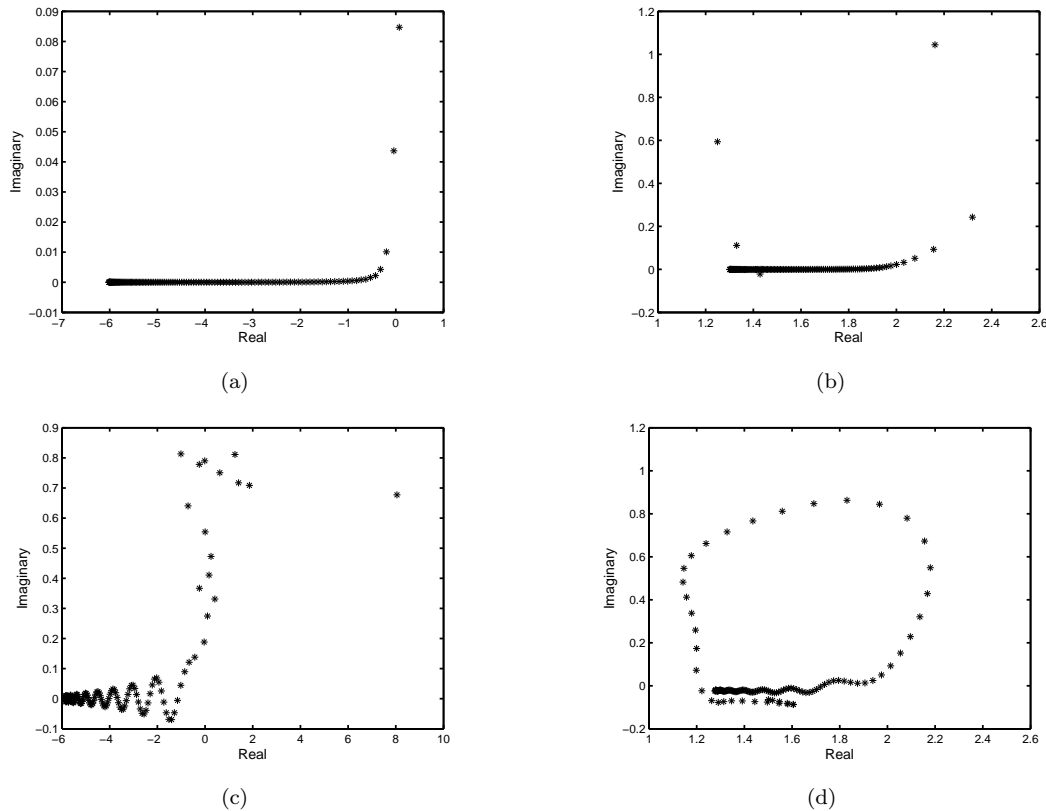


Fig. 4.1. The eigenvalues distribution of the unpreconditioned B and preconditioned $M^{-1}B$ for the cavity filled with the medium of $\epsilon_r = 4 + i$ with 128×128 meshes when $k = 2\pi$ and 16π separately in the TM case.

To verify the effectiveness of the preconditioner M^{-1} , the eigenvalue distributions of the preconditioned coefficient matrix $M^{-1}B$ for the cavity filled with the medium of $\epsilon_r = 4 + i$ are shown for different wave numbers in Figs. 4.1 and 4.2. In Fig. 4.1, (a) and (c) show the eigenvalue distribution of unpreconditioned coefficient matrix with $N = M = 128$ for $k = 2\pi$ and 16π respectively, and it can be seen that some of the real parts of the eigenvalues cluster

around zero, and some are negative. This phenomenon is more obvious in Fig. 4.2, which show the eigenvalue distributions of unpreconditioned (in (a) and (c)) and preconditioned linear system (in (b) and (d)) with $N = M = 1024$ for $k = 100\pi, 300\pi$. After making use of the preconditioner M^{-1} , in (b) and (d) of Figs. 4.1 and 4.2, the real parts of the eigenvalues of coefficient matrix are positive, and the ratio of the maximum and minimum of the eigenvalues, which denotes the condition number of the linear system, has drastically decreased. All of these have improved the convergence behavior of the iterative methods to a large extent. This can also be observed from Table 4.1 in detail. The preconditioner is very efficient for cavity model with large wave numbers while using the non-preconditioning method a large number of iteration is needed to get the convergent solution, even the iteration is not convergent, e.g., for $k = 300\pi$ with 512×512 meshes.

We testified the convergence order of the presented method in Table 4.2, where we consider the case of empty cavity for $k = 8\pi, 16\pi, 32\pi, 64\pi$ and the cavity filled with the medium $\epsilon_r = 4+i$ for $k = 4\pi$, and the convergence order is taken as

$$\text{Order} = \frac{\log\left(\frac{e_{h_1}}{e_{h_2}}\right)}{\log\left(\frac{h_1}{h_2}\right)}.$$

It can be evidently observed that the proposed method is fourth order accurate. To be more

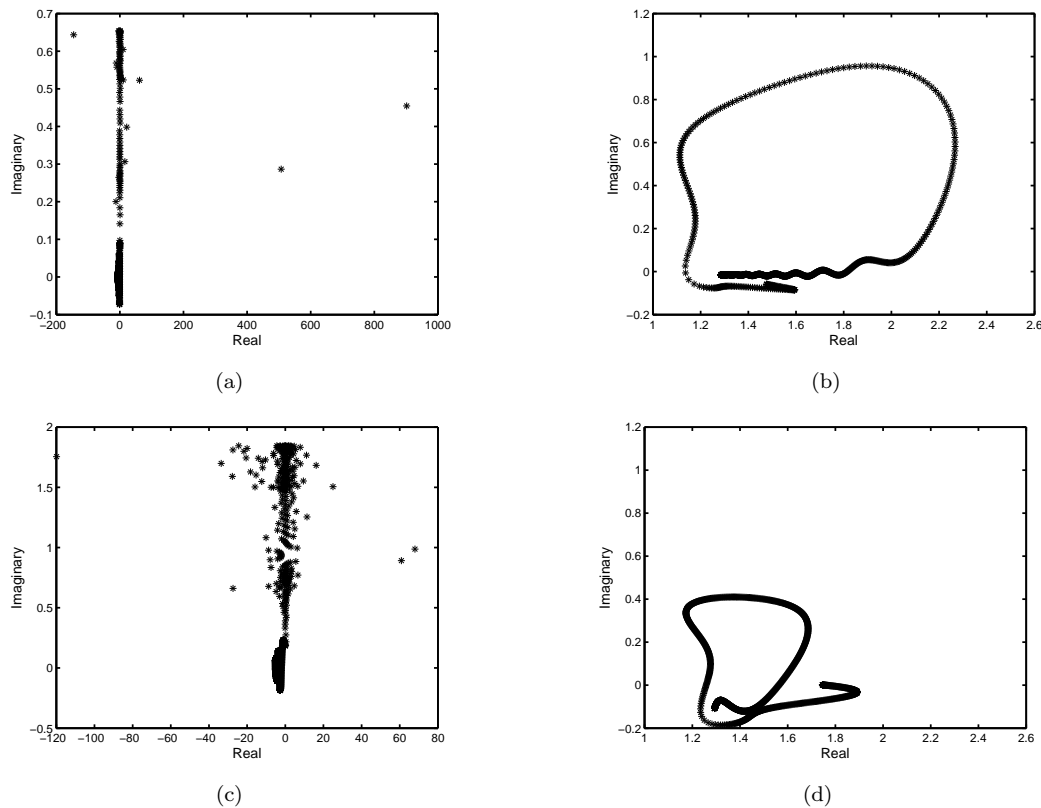
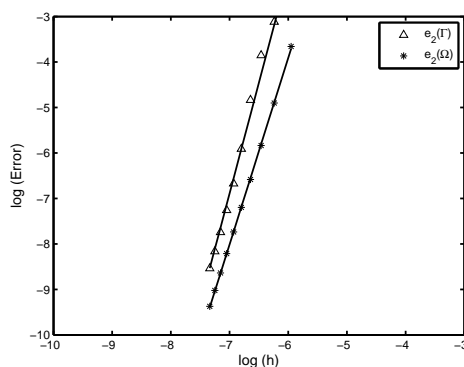


Fig. 4.2. The eigenvalues distribution of the unpreconditioned B and preconditioned $M^{-1}B$ for the cavity filled with the medium of $\epsilon_r = 4+i$ with 1024×1024 meshes when $k = 100\pi$ and 300π separately in the TM case.

Table 4.1: Comparison of the eigenvalues of the preconditioned and unpreconditioned coefficient matrix for the cavity filled with the medium of $\varepsilon_r = 4 + i$ with the fourth order discretization.

k_0	$M = N$	Preconditioned				Unpreconditioned			
		Iter	$\min \lambda_i $	$\max \lambda_i $	$\frac{\max \lambda_i }{\min \lambda_i }$	Iter	$\min \lambda_i $	$\max \lambda_i $	$\frac{\max \lambda_i }{\min \lambda_i }$
2π	128	10	1.3019	2.4006	1.8440	44	0.0599	6.0122	100.29
	256	10	1.3022	2.4162	1.8555	63	0.0302	6.0146	199.19
	512	10	1.3023	2.4238	1.8611	91	0.0152	6.0151	396.97
	1024	10	1.3024	2.4275	1.8639	131	0.0076	6.0153	792.54
16π	128	14	1.2006	2.2582	1.8809	85	0.1917	8.0799	42.143
	256	15	1.1756	2.4694	2.1005	131	0.1038	5.9712	57.500
	512	16	1.1636	2.5668	2.2059	188	0.0543	6.0043	110.57
	1024	16	1.1576	2.6110	2.2555	300	0.0278	6.0126	216.39
100π	512	12	1.1818	2.0163	1.7061	354	0.1944	114.04	586.74
	1024	14	1.1363	2.3626	2.0793	450	0.0992	901.88	9092.1
300π	512	7	1.1479	1.4708	1.2813	> 1190	0.2603	2289.4	8795.2
	1024	10	1.2186	1.8919	1.5526	745	0.1873	119.90	639.98

Fig. 4.3. The log-log plot of the error $e_2(\Gamma)$ (Δ) and $e_2(\Omega)$ ($*$) versus the mesh spacing h . The solid lines are the linear least squares fittings whose slopes are the average orders of accuracy which is 4.8671 for $e_2(\Gamma)$ and 4.1006 for $e_2(\Omega)$.

precise about the convergence order, for $k = 300\pi$, $\varepsilon_r = 4 + i$, we use a linear squares fitting to find the average order of accuracy using

$$\log(\text{Error}) \approx \text{Order} \log\left(\frac{1}{N}\right) + C$$

in Fig. 4.3. We choose $N = 384 + 128k$, $k = 0, 1, 2, \dots, 9$. The order is found to be 4.8671 for $e_2(\Gamma)$ and 4.1006 for $e_2(\Omega)$.

We also consider the layered media defined by

$$\varepsilon_r(x, y) = \begin{cases} 1, & -\frac{b}{4} \leq x \leq 0, \\ 2, & -\frac{b}{2} \leq x < -\frac{b}{4}, \\ 16 + i, & -\frac{3b}{4} \leq x < -\frac{b}{2}, \\ 1.5, & -b/ \leq x < -\frac{3b}{4}. \end{cases} \quad (4.1)$$

The numerical results by the second order scheme and the proposed fourth order scheme are listed in Table 4.3. It is observed that the proposed high order scheme yields nearly fourth

order accuracy even without any treatment on the interface for the layered media. The reason may be that the constructed solution is very smooth, and the solution and its second order derivatives do not have jumps. As only the wave number k has jumps, the local truncation error is $\mathcal{O}(h^2)$ at the interface, but $\mathcal{O}(h^4)$ on all other points. So from the analysis in [21], we know the convergence rate should be $\mathcal{O}(h^3)$ for a curve interface. However, as the interface is a straight line in our case, some terms will be canceled out during the Taylor expansion procedure. A similar higher order phenomenon was analyzed for one-dimensional problem in [4]. This may explain the observation of the convergence order higher than the theoretical estimate.

Table 4.2: Errors for Example 1 by the fourth order algorithm.

k_0	Error	Meshes				Order
		128×128	256×256	512×512	1024×1024	
8π	$e_M(\Gamma)$	$3.4543e-06$	$2.1566e-07$	$1.3472e-08$	$8.4240e-10$	$h^{4.0005}$
	$e_2(\Gamma)$	$1.8234e-06$	$1.1377e-07$	$7.1057e-09$	$4.4438e-10$	$h^{4.0008}$
	$e_M(\Omega)$	$8.5228e-06$	$5.3562e-07$	$3.3511e-08$	$2.0966e-09$	$h^{3.9964}$
	$e_2(\Omega)$	$3.2193e-06$	$2.0090e-07$	$1.2548e-08$	$7.8424e-10$	$h^{4.0011}$
16π	$e_M(\Gamma)$	$6.5289e-05$	$4.0707e-06$	$2.4511e-07$	$1.5877e-08$	$h^{4.0019}$
	$e_2(\Gamma)$	$3.6142e-05$	$2.2545e-06$	$1.4087e-07$	$8.8053e-09$	$h^{4.0010}$
	$e_M(\Omega)$	$1.2776e-04$	$8.0675e-06$	$5.0576e-07$	$3.1646e-08$	$h^{3.9930}$
	$e_2(\Omega)$	$3.7853e-05$	$2.3649e-06$	$1.4790e-07$	$9.2486e-09$	$h^{3.9996}$
32π	$e_M(\Gamma)$	$9.0463e-04$	$5.5019e-05$	$3.4010e-06$	$2.1131e-07$	$h^{4.0213}$
	$e_2(\Gamma)$	$5.3045e-04$	$3.1946e-05$	$1.9729e-06$	$1.2271e-07$	$h^{4.0259}$
	$e_M(\Omega)$	$1.8000e-03$	$1.1393e-04$	$7.1364e-06$	$4.4733e-07$	$h^{3.9915}$
	$e_2(\Omega)$	$3.7274e-04$	$2.2401e-05$	$1.3842e-06$	$8.6137e-08$	$h^{4.0264}$
64π	$e_M(\Gamma)$	$7.8000e-03$	$4.3901e-04$	$3.0451e-05$	$1.9409e-06$	$h^{3.9908}$
	$e_2(\Gamma)$	$5.1000e-03$	$1.6203e-04$	$1.1690e-05$	$7.5764e-07$	$h^{4.2389}$
	$e_M(\Omega)$	$2.6200e-02$	$1.7000e-03$	$1.1066e-04$	$6.9446e-06$	$h^{3.9605}$
	$e_2(\Omega)$	$4.5000e-03$	$3.5064e-04$	$2.2692e-05$	$1.4327e-06$	$h^{3.8723}$
4π $4+i$	$e_M(\Gamma)$	$2.7234e-07$	$1.6905e-08$	$1.0532e-09$	$6.5571e-11$	$h^{4.0067}$
	$e_2(\Gamma)$	$1.6551e-07$	$1.0271e-08$	$6.3977e-10$	$3.9816e-11$	$h^{4.0071}$
	$e_M(\Omega)$	$1.2255e-06$	$7.7096e-08$	$4.8329e-09$	$3.0231e-10$	$h^{3.9950}$
	$e_2(\Omega)$	$2.0943e-07$	$1.3045e-08$	$8.1393e-10$	$5.0766e-11$	$h^{4.0034}$

Table 4.3: Errors for the solutions of Example 1 of the cavity filled with layered media (4.1) by the 2nd order scheme and the proposed algorithm.

Method	k_0	Error	Meshes			Order
			128×128	256×256	512×512	
second order	4π	$e_2(\Gamma)$	$9.6031e-05$	$2.4938e-05$	$6.5645e-06$	1.9353
		$e_2(\Omega)$	$1.8431e-04$	$4.5277e-05$	$1.1438e-05$	2.0051
	16π	$e_2(\Gamma)$	$2.6602e-03$	$6.6559e-04$	$1.6415e-04$	2.0092
		$e_2(\Omega)$	$1.9100e-03$	$4.7936e-04$	$1.2226e-04$	1.9944
	64π	$e_2(\Gamma)$	$1.0914e-02$	$3.4200e-03$	$6.7398e-04$	2.0087
		$e_2(\Omega)$	$3.2991e-02$	$8.3633e-03$	$2.0826e-03$	1.9916
fourth order	4π	$e_2(\Gamma)$	$8.3500e-08$	$5.4024e-09$	$3.4361e-10$	3.9624
		$e_2(\Omega)$	$1.3304e-07$	$8.3853e-09$	$5.3676e-10$	3.9767
	16π	$e_2(\Gamma)$	$1.6443e-05$	$1.0328e-06$	$6.5806e-08$	3.9825
		$e_2(\Omega)$	$1.7499e-05$	$1.1554e-06$	$7.3394e-08$	3.9487
	64π	$e_2(\Gamma)$	$7.0315e-03$	$4.6567e-04$	$2.9844e-05$	3.9401
		$e_2(\Omega)$	$7.4880e-08$	$4.7034e-09$	$2.9473e-10$	3.9414

Remark 4.1. If the second order derivatives of the solution have jumps at the interfaces of the layered media, both the second order and fourth order scheme will only result in the first order accuracy. The Helmholtz interior problem with this kind of solution has been considered in [26].

4.2. Example 2

Another artificial example defined by (2.5a) with a cavity $a = b = 1$ is used to verify the accuracy of approximations. The $f(x, y)$ and $g(x)$ are chosen such that the exact function is

$$u(x, y) = (1 + i)\sin\left(\frac{k_0 x}{2}\right)\sin\left(\frac{(k_0 - \pi)(y + 1)}{2}\right),$$

and $g(x)$ is computed by $g(x) = \frac{\partial u}{\partial n} - I(u)$.

In Table 4.4, we report the results, including the errors and CPU time, for second order and fourth order computations with 4, 8, 16, 32, 64, 128 and 256 points per wavelength (λ/h) when $k_0 = 8\pi$. As seen in the table, the proposed method is fourth order accurate. The fourth order method obtained much more accurate solutions than the second order algorithm by costing almost the same CPU time with the same mesh density. The solution computed by the fourth order scheme with 16 points per wavelength is comparable to that computed by the second

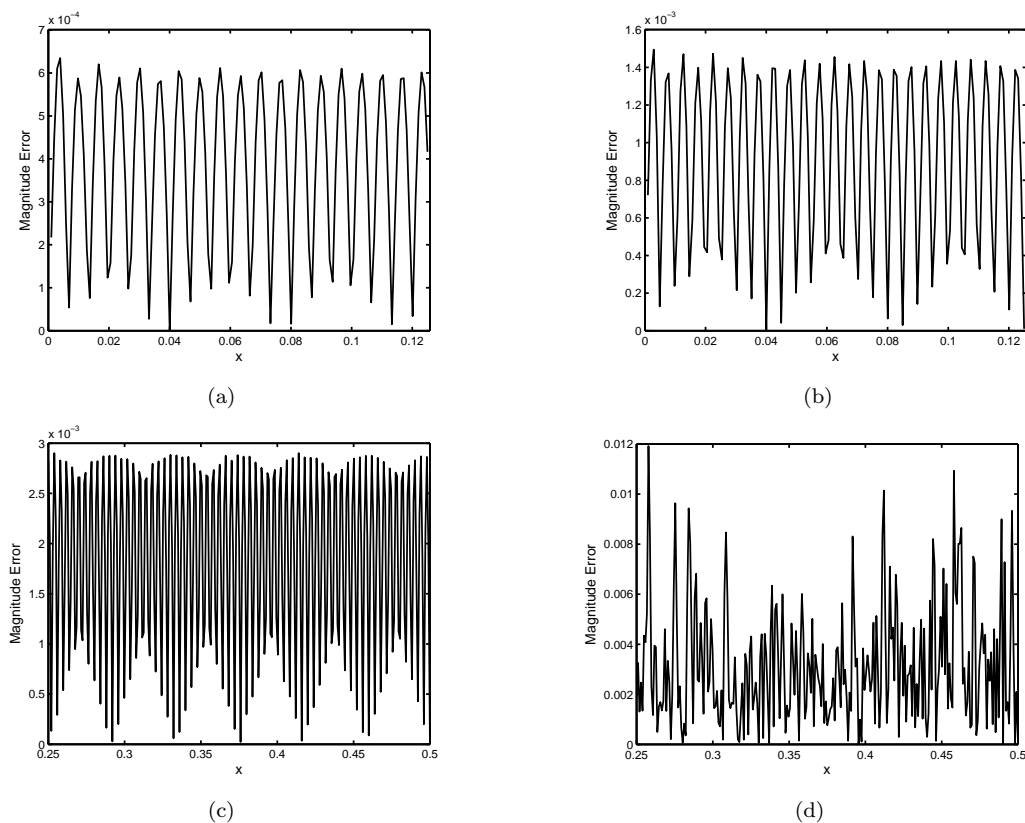


Fig. 4.4. The error distribution at the aperture of the empty cavity for $k = 300\pi, 400\pi, 500\pi, 600\pi$ in (a), (b), (c) and (d) separately with 1024×1024 meshes.

order scheme with 256 points per wavelength. So much CPU time can be saved with our fourth order method to get the same accurate solution.

Finally, for large wave numbers, such as $k = 300\pi, 400\pi, 500\pi, 600\pi$, the errors of the solutions on the part of the boundary Γ are displayed with 1024×1024 meshes in (a-d) of Fig. 4.4 separately, $x \in [0, 0.125]$ in (a) and (b), and $x \in [0.25, 0.5]$ in (c) and (d). The proposed algorithm gives excellent accuracy for relatively large k .

Table 4.4: Errors and CPU time (sec.) for Example 2 by the second and the fourth order algorithm with $k_0 = 8\pi$.

Meshes	λ/h	second order			fourth order		
		$e_2(\Omega)$	Order	CPU	$e_2(\Omega)$	Order	CPU
16^2	4	$1.9854e-02$		0.031	$2.6579e-03$		0.043
32^2	8	$8.2621e-03$	1.2648	0.094	$1.5206e-04$	4.1276	0.125
64^2	16	$1.6799e-03$	2.2981	0.359	$9.4527e-06$	4.0078	0.328
128^2	32	$3.8917e-04$	2.1099	1.219	$5.9211e-07$	3.9968	1.188
256^2	64	$9.6122e-05$	2.0125	6.047	$3.7080e-08$	3.9972	5.594
512^2	128	$2.3975e-05$	2.0033	25.25	$2.3103e-09$	4.0045	27.51
1024^2	256	$5.9922e-06$	2.0004	141.0	$1.4420e-10$	4.0019	150.5

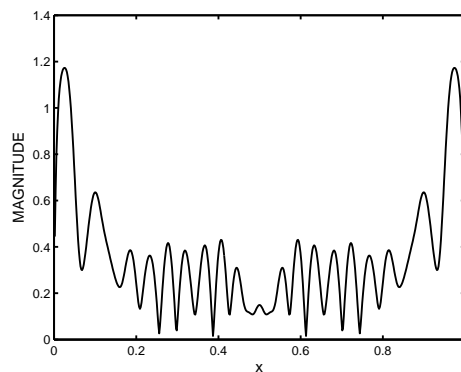


Fig. 4.5. Magnitude of the aperture field at normal incidence with homogeneous medium $\varepsilon_r = 1.0$ when $k_0 = 32\pi$.

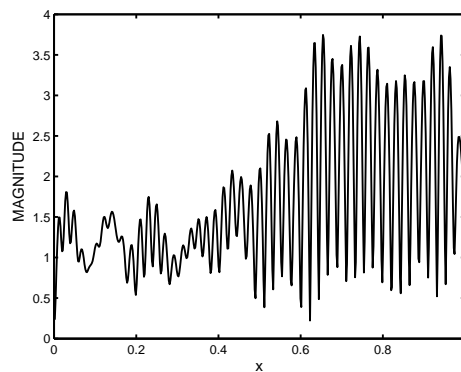


Fig. 4.6. Magnitude of the aperture field at $\theta = \pi/4$ with homogeneous medium $\varepsilon_r = 1.0$ when $k_0 = 64\pi$.

4.3. Example 3

Consider a plane wave scattering from a rectangular groove with 1 meter wide and 0.25 meter deep at normal incidence. We applied the presented fourth order scheme to discrete the model, and the preconditioned BICGstab method to solve the last linear system. The magnitude and phase of the field of the cavity filled with the medium $\varepsilon_r = 1.0$ and $\varepsilon_r = 4.0 + i$ are given, and the interesting physical parameter, the radar cross section (RCS) is also computed in Fig. 4.7, in which the numerical results by the fourth order method are compared with those results, indicated by 'o', obtained by the finite element method in [6]. For some large k such as 32π , 64π , the numerical results are given in Figs. 4.5 and 4.6, in which high oscillation of the solution is clearly displayed.

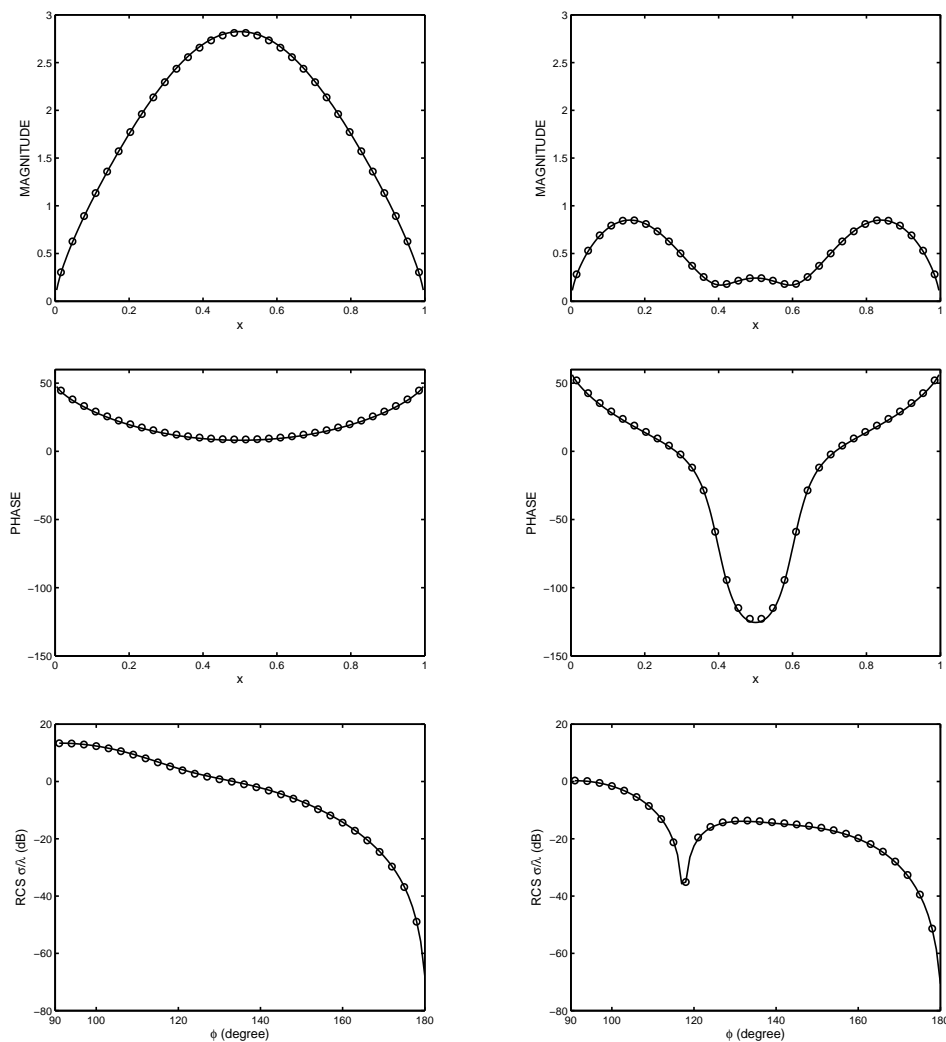


Fig. 4.7. The magnitude and phase of the aperture of electric field at normal incidence and the backscatter RCS for the empty cavity ($\varepsilon_r = 1.0$) and the filled cavity ($\varepsilon_r = 4.0 + i$) in the TM case when $k_0 = 2\pi$.

5. Conclusions and Future Work

In this paper, a fast high order method has been presented for the analysis of the scattering from open rectangular cavities. In the interior of the domain, a compact fourth order scheme is used to discretize the Helmholtz equation, and a special treatment is enforced on the nonlocal boundary, which yields that the truncation errors in $\bar{\Omega}$ reach $\mathcal{O}(h^4)$. The fast algorithm is presented to reduce the resulting discrete system to an interface linear system employing the discrete Fourier transform in the horizontal direction and the Gaussian elimination in the vertical direction. An effective preconditioner for the BICGstab iterative solver is proposed to improve the condition number of the interface linear system, which further raises the efficiency of the presented fourth order algorithm. Numerical experiments showed that the proposed method could obtain higher accurate solutions with less mesh points, which can lead to a remarkable saving in the computation cost. The scheme with about four points per wavelength sufficiently well approximate the oscillatory solution for the large wave number k , such as 400π , 500π . For the cavity model in which the second order derivatives of the solution are discontinuous in the domain, some special treatments on the interfaces between the layered media are needed to get the higher order accuracy, such as using the immerse interface method. It will be presented in our future work.

Acknowledgments. The research of the second author was supported by the FRG grant of the Hong Kong Baptist University (No. FRG/08-09/II-35). The research of the third author was supported by the FRG grant of the Hong Kong Baptist University, the GIF Grants of Hong Kong Research Grants Council, and the Collaborative Research Fund of National Science Foundation of China (NSFC) under Grant No. G10729101.

References

- [1] H. Ammari, G. Bao and A. W. Wood, Analysis of the electromagnetic scattering from a cavity, *Japan J. Indust. Appl. Math.*, **19** (2002), 301-310.
- [2] A. Wood, Analysis of electromagnetic scattering from an overfilled cavity in the ground plane, *J. Comput. Phys.*, **215** (2006), 630-641.
- [3] G. Bao and W. Sun, A fast algorithm for the electromagnetic scattering from a large cavity, *SIAM J. Sci. Comput.*, **27** (2005), 553-574.
- [4] R. P. Beyer and R. J. LeVeque, Analysis of one-dimensional model for the immersed boundary method, *SIAM J. Numer. Anal.*, **29** (1992), 332-364.
- [5] J. Huang, A. W. Wood and M. J. Havrilla, A hybrid finite element-Laplace transform method for the analysis of transient electromagnetic scattering by an over-filled cavity in the ground plane. *Commun. Comput. Phys.*, **5** (2009), 126-141.
- [6] J. Jin, *The Finite Element Method in Electromagnetics*, John Willey Sons, New York, 1993.
- [7] J. Liu and J. Jin, A special higher order finite-element method for scattering by deep cavities, *IEEE Trans. Antennas Propag.*, **48** (2000), 694-703.
- [8] J. Jin, J. Liu, Z. Lou and S. Liang, A fully high-order finite-element simulation of scattering by deep cavities, *IEEE Trans. Antennas Propag.*, **51** (2003), 2420-2429.
- [9] Z. Xiang and T. Chia, A hybrid BEM-WTM approach for analysis of the EM scattering from large open-ended cavities, *IEEE Trans. Antennas Propag.*, **49** (2001), 165-173.
- [10] D. Zhang, F. Ma and H. Dong, A finite element method with rectangular perfectly matched layers for the scattering from cavities, *J. Comput. Math.*, **26** (2008), 98-111.
- [11] K. Ito, Z. Qiao and J. Toivanen, A domain decomposition solver for acoustic scattering by elastic objects in layered media, *J. Comput. Phys.*, **227** (2008), 8685-8698.

- [12] Q. Fang, D. P. Nicholls and J. Shen, A stable, high-order method for three-dimensional, bounded-obstacle, acoustic scattering, *J. Comput. Phys.*, **224** (2007), 1145-1169.
- [13] Y. Fu, Compact fourth-order finite difference schemes for Helmholtz equation with high wave numbers, *J. Comput. Math.*, **26** (2008), 98-111.
- [14] Y. Wang, K. Du and W. Sun, A second-order method for the electromagnetic scattering from a large cavity, *Numer. Math. Theor. Meth. Appl.*, **1** (2008), 357-382.
- [15] J. Wu, Y. Wang, W. Li and W. Sun, Toeplitz-type approximations to the Hadamard integral operators and their applications in electromagnetic cavity problems, *Appl. Numer. Math.*, **58** (2008), 101-121.
- [16] B. Gustafsson and E. Mossberg, Time compact high order difference methods for wave propagation, *SIAM J. Sci. Comput.*, **26** (2004), 259-271.
- [17] G. Baruch, G. Fibich, S. Tsynkov and E. Turkel, Fourth order schemes for time-harmonic wave equations with discontinuous coefficients, *Commun. Comput. Phys.*, **5** (2009), 442-455.
- [18] B. Gustafsson and P. Wahlund, Time compact difference methods for wave propagation in discontinuous media, *SIAM J. Sci. Comput.*, **26** (2004), 272-293.
- [19] B. Gustafsson and P. Wahlund, Time compact high order difference methods for wave propagation, 2D, *J. Sci. Comput.*, **25** (2005), 195-211.
- [20] Q. Huynh, K. Ito and Z. Qiao, High order finite difference schemes for wave equations in heterogeneous media, *In preparation*.
- [21] R. J. LeVeque and Z. Li, The immersed interface method for elliptic equations with discontinuous coefficients and singular sources, *SIAM J. Numer. Anal.*, **31** (1994), 1019-1044.
- [22] F. Ihlenburg. Finite Element Analysis of Acoustic Scattering, In Vol. 132 of *Applied Mathematical Sciences*, Springer-Verlag, New York, 1998.
- [23] F. Ihlenburg and I. Babuska, Finite element solution of the Helmholtz equation with high wave number Part I: The h -version of FEM, *Comput. Math. Appl.*, **30** (1995), 9-37.
- [24] F. Ihlenburg and I. Babuska, Finite element solution of the Helmholtz equation with high wave number Part II: The h - p version of the FEM, *SIAM J. Numer. Anal.*, **34** (1997), 315-358.
- [25] G. Baruch, G. Fibich and S. Tsynkov, High-order numerical method for the nonlinear Helmholtz equation with material discontinuities, *J. Comput. Phys.*, **227** (2007), 820-850.
- [26] X. Feng, Z. Qiao and Z. Li, High order compact finite difference schemes for Helmholtz equation with discontinuous coefficient, *accepted by J. Comput. Math.*